Agricultural and Forest Meteorology 372 (2025) 110679

Contents lists available at ScienceDirect

Agricultural and Forest Meteorology

journal homepage: www.elsevier.com/locate/agrformet

# Beyond meteorological data: Modelling tree growth with ERA5-Land

Marian Schönauer [a,*], Christoph Pucher [b], Jan Altman [c,d,e], Josef Weißbacher [f], Lars Sprengel [g], Boris Rewald [a]

[a] Department of Forest Protection and Wildlife Management, Faculty of Forestry and Wood Technology, Mendel University in Brno, 61300 Brno, Czech Republic
[b] Department of Ecosystem Management, Climate and Biodiversity, Institute of Silviculture, BOKU University, 1190 Vienna, Austria
[c] Institute of Botany, The Czech Academy of Sciences, 37901 Třeboň, Czech Republic
[d] Faculty of Forestry and Wood Sciences, Czech University of Life Sciences, 16521 Prague, Czech Republic
[e] Department of Geography, Institute of Ecology and Earth Sciences, University of Tartu, Vanemuise 46, 51003 Tartu, Estonia
[f] Ziviltechnikerbüro Weissbacher, 6313 Wildschönau, Austria
[g] Department of Silviculture and Forest Ecology of the Temperate Zones, University of Göttingen, 37077 Göttingen, Germany

ARTICLE INFO

*Keywords:*
Earth observation
Climate reanalysis data
Climate-vegetation interactions
Dendrochronology
Forest growth modelling
Tree-ring width

ABSTRACT

Forests are increasingly impacted by climate change, affecting tree growth and carbon sequestration. Tree-ring width, closely related to tree growth, is a key climate proxy, yet models describing ring width or growth often lack comprehensive environmental data. This study assesses ERA5-Land data for tree-ring width prediction compared to automatic weather station observations, emphasizing the value of extended and global climate data.

We analyzed 723 site-averaged and detrended tree-ring chronologies from two broadleaved and two gymnosperm species across Europe, integrating them with ERA5-Land climate data, $CO_2$ concentration, and a drought index (SPEI12). A subset was compared with weather station data. For modelling interannual variations of tree-ring width we used linear models to assess parameter importance.

ERA5-Land and weather-station-based models performed similarly, maintaining stable correlations and consistent errors. Models based on meteorological data from weather stations highlighted SPEI12, sunshine duration, and temperature extremes, while ERA5-Land models emphasized SPEI12, dew-point temperature (humidity), and total precipitation. $CO_2$ positively influenced the growth of gymnosperm species. ERA5-Land facilitated broader spatial analysis and incorporated additional factors like evaporation, snow cover, and soil moisture. Monthly assessments revealed the importance of parameters for each species.

Our findings confirm that ERA5-Land is a reliable alternative for modeling tree growth, offering new insights into climate-vegetation interactions. The ready availability of underutilized parameters, such as air humidity, soil moisture and temperature, and runoff, enables their inclusion in future growth models. Using ERA5-Land can therefore deepen our understanding of forest responses to diverse environmental drivers on a global scale.

## 1. Introduction

Temperate and boreal forest ecosystems are exposed to an increasingly warmer and often drier climate (IPCC, 2023). While some forest ecosystems may benefit from an extended growing season, drought has become a major growth constraint, fostering mortality (Senf et al., 2020) and reducing growth (Bose et al., 2024; Vicente-Serrano et al., 2014). Growth and the underlying physiological processes that support photosynthesis, cambial activity and xylogenesis (Schweingruber, 2007) are under direct environmental control, in particular by temperature and hydroclimatic conditions (Etzold et al., 2014; Martínez-Fernández et al., 2019). Tree-ring width (TRW) provide important long-term evidence of how tree growth responded to the past environment (Anderegg et al., 2015; Kannenberg et al., 2020; Schweingruber, 2012; Jeong et al., 2021). As tree species exhibit a wide variety of growth rates, water use strategies, and ability to tolerate low/high temperatures and droughts (Obladen et al., 2021; Serra-Maluquer et al., 2022), species-specific patterns in climate response of tree growth are required (Babst et al., 2013). Furthermore, TRW data contain age- and size-related trends (Weiner and Thomas, 2001), $CO_2$ fertilisation effects (Arco Molina et al., 2024; Keenan et al., 2013), biological memory effects including drought legacies (Anderegg et al., 2015; Bose et al., 2024; Kannenberg et al.,

* Corresponding author.
*E-mail address:* marian.schoenauer@mendelu.cz (M. Schönauer).

https://doi.org/10.1016/j.agrformet.2025.110679
Received 2 April 2025; Received in revised form 26 May 2025; Accepted 30 May 2025
Available online 7 June 2025

2020), and perturbations and other properties at stand level (management, insect outbreaks, etc.; (Altman et al., 2013; Sedjo and Sohngen, 2012)).

With anticipated fluctuations in climate conditions (Berg and Sheffield, 2018), an accurate representation of growing conditions will be of increasing importance to predict future forest development (Tang et al., 2024). Different types of forest growth models exist and are becoming essential tools in research, management, and policymaking (Blanco and Lo, 2023). For example, process-based forest growth models commonly applied at smaller scales (e.g. Gupta and Sharma, 2019; Härkönen et al., 2019) integrate site information, and derive current growing conditions from meteorological data. Applicability of these models depends heavily on climate time series traditionally provided by automatic weather stations ('AWS') (WMO, 2023). Networks such as the 'Remote Automated Weather Station' (Western Regional Climate Center, 2008), and the 'European Climate Assessment&Dataset' ('ECA&D' or 'E-OBS') (Klein Tank et al., 2002) already provide platforms on a large scale, although the access to larger amounts of data can be challenging. In other regions meteorological data are scattered across national agencies, not synchronized and of limited availability; many remote sites are still not covered by surface observations (Sabatini, 2017). Other limitations include the highly variable temporal coverage by AWS (Capra et al., 2013; Castellanos-Acuna and Hamann, 2020), compounded by the decommissioning of stations or cessation of specific measurements. In turn, the available data vary in the degree of information provided (Pelosi et al., 2021). Readily available data on evapotranspiration or belowground parameters such as soil moisture, which are considered increasingly important for modelling climate-vegetation feedbacks (Balting et al., 2021; Jaafar and Sujud, 2024), are lacking. As a result, most process-based growth models use, for example, basic water balances obtained as the difference between total evapotranspiration and precipitation (Gupta and Sharma, 2019; Härkönen et al., 2019; Lexer and Hönninger, 2001), while advanced parameters such as winter soil water storage or delayed runoff from snow (Swann et al., 2016) cannot usually be considered. This may limit the performance of (tree) growth models under changing climate conditions (Bugmann, 2001) and hinder the modelling of more specific processes (e.g. regeneration, root growth (Blanco and Lo, 2023)). Therefore, standardized meteorological and bioclimatic datasets beyond the current limitations of AWS parameters are urgently needed to facilitate further development of accurate tree growth models under global change.

Such comprehensive and ready-to-use sets of parameters can be provided by gridded data from assimilations or reanalysis, created by merging and scaling of satellite observations and *in-situ* data, including E-OBS (e.g. Muñoz-Sabater et al., 2021). In turn, they provide a reliable basis for monitoring large areas at high spatial and temporal resolution including available soil water (Muñoz-Sabater et al., 2021). Gridded climate data products are increasingly used to quantify the effects of climate change on forest growth and to forward modelling over large spatial gradients (e.g. Jevšenak et al., 2024; Martínez-Fernández et al., 2019; Wang et al., 2024). The ERA5-Land dataset, recently refined to a grid cell size of 9 km, provides a consistent view on multiple climate parameters since 1950 (Muñoz-Sabater et al., 2021). It is a replay of the land component of the ERA5 climate reanalysis, which assimilates as many observations as possible in the upper air and near surface (C3S, 2024a). Estimates of ERA5-Land have already been validated and show a good agreement with *in-situ* measurements, particular in the description of hydrological parameters (Lal et al., 2022; Schönauer et al., 2025). ERA5-Land provides open access data with multiple access options through online data queries, API (C3S, 2024) and an R-package (Hufkens, 2019).

However, it is not known whether ERA5-Land climate parameters can replace meteorological data from weather stations for use in tree growth modelling. Here we aim to assess the suitability of the two sources of climate data for modelling the annual tree-ring width (TRW) of four major tree species across Europe. In this work we

1. Modelled and predicted tree growth using meteorological data from weather stations, and with data available from ERA5-Land (using a weather station subset or the full dataset of chronologies for comparisons),
2. Identified independent variables that contribute to tree growth modelling for both climate datasets at monthly resolution.

## 2. Material and methods

For this study, we used tree-ring data of two deciduous broadleaved (Sessile oak and European beech) and two gymnosperm tree species (Norway spruce and Scots pine) with high occurrences in Europe (FOREST EUROPE, 2020). The TRW data was merged with meteorological data from weather stations, or with climate data from ERA5-Land. Linear models were employed to model annual changes of detrended TRW values with the environmental data added. The coefficients of the models were used to identify the importance of the environmental parameters, and the model residuals were analysed to determine the influence of the distance to the nearest available weather station.

### 2.1. Dendrochronological data

Tree-ring data from Norway spruce (*Picea abies* (L.) H. Karst.), Scots pine (*Pinus sylvestris* L.), Sessile oak (*Quercus petraea* (Matt.) Liebl.), and European beech (*Fagus sylvatica* L.), which are among the most ecologically and economically important tree species across Europe, and particularly in Central Europe (Leuschner and Ellenberg, 2017), were based on two sources: (I) the International Tree-ring Data Bank ('ITRDB', Grissino-Mayer and Fritts, 1997; details in Zhao et al., 2019) and (II) tree cores generated during forest inventories, covering different site conditions and biogeoclimatic regions across Europe (Fig. 1). (I) The ITRDB provides data for the selected species from >36,000 trees and ~1000 sites, with most data generally (~81 % of sites) available for conifer stands incl. *P. sylvestris* ($2^{nd}$) and *P. abies* ($5^{th}$). Among broadleaves, sample sites in the ITRDB are dominated by *Quercus* spp. (~14 %) followed by *Fagus sylvatica* (~5 %). We used the cleaned version of the database (Guiterman et al., 2024; Zhao et al., 2019). TRW data for selected species of continental Europe was retrieved by downloading all available observations on 'total ring width' from the ITRDB (NOAA, 2025). Although the ITRDB has a shortage of metadata, associated benefits in terms of coverage and accessibility motivate its use; see Supplementary Table 1 for used TRW sources. (II) Since the Alpine western region of Austria was underrepresented for *P. abies* in the ITRDB, we also employed tree cores of *P. abies*, collected during forest inventories between 2014 and 2023 in Tyrol, Austria. These inventories consisted of median basal area trees selected based on the methodology of angle-count samplings (Bitterlich, 1952); a subset of 159 trees from 14 sites was randomly selected for analyses. The tree cores sampled in Tyrol were extracted upslope at breast height (130 cm) from each tree. The samples were air-dried, glued onto wooden laths, and sanded (finest granularity was 240) to improve ring visibility. High resolution scans (1200 ppi) were made using a graphic scanner (EPSON 10000XL, Epson, Japan). These images were analysed using the software tools CooRecorder for actual tree-ring measurements and CDendro for initial crossdating (Cybis Elektronik & Data AB, Saltsjöbaden, Sweden; v. 9.8.1).

Raw values of all tree-ring series were detrended with an age-dependent spline ('AgeDepSpline') with an initial stiffness of 50, using the package 'dplR' (Bunn et al., 2024; Bunn, 2010, 2008) in R (R Core Team, 2024). The AgeDepSpline detrending method applies an age-dependent cubic smoothing spline to each tree-ring series. Starting with a stiffness of 50, the spline becomes progressively more rigid with each measurement. This allows the flexible spline to capture the larger growth of young trees and the rigid spline to model the smaller, steadier growth of mature trees. Where negative fits occurred, the method 'mean'

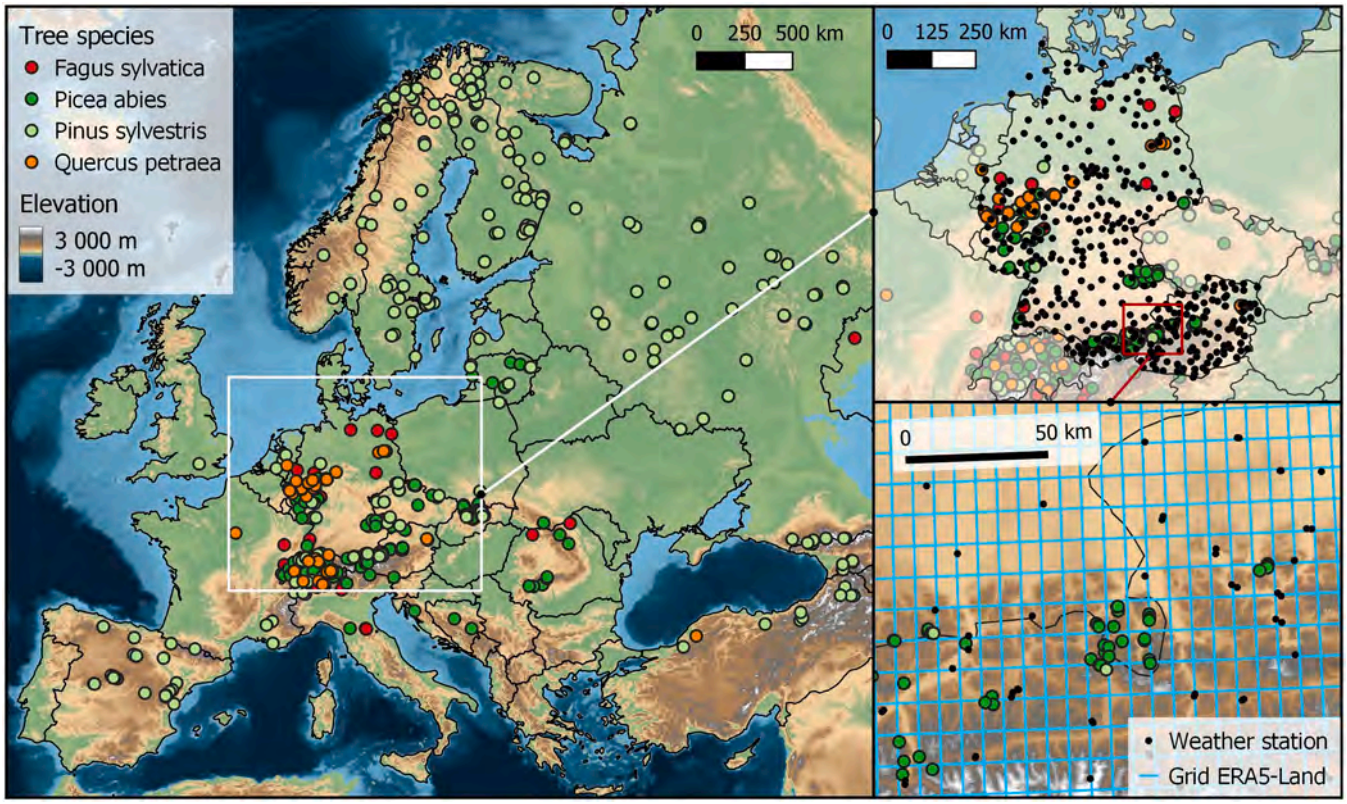


**Fig. 1.** The main map shows colour-coded stands of four tree species included in the tree-ring width dataset ($TRW_{all}$), details of Austria and Germany ($TRW_{AWS}$) with automatic weather stations (AWS, black dots; top right), and an example overlay of ERA5-Land grid cells (blue lines), locations of AWS and sites (bottom right). The ACE2 (Altimeter Corrected Elevations, v.2) digital elevation model is used as the background (Berry et al., 2018). Note: different scales of maps.

was used, which fits a horizontal line using the mean of the series. To describe the responses of species' TRW to various environmental parameters, a stand-level analysis is more informative than an analysis of individual trees (Speer, 2009). Since all trees were clustered into sites, a biweighted robust estimation of the mean, which is unaffected by outliers and thus reduces error variance, was applied to construct mean value chronologies for each site and species (Cook and Kairiukstis, 1992). These chronologies were calculated when at least 3 tree-individual TRW series with a minimum length of 50 years could be used per site (sites with fewer trees were excluded). The chronologies were truncated to the period between 1950 and 2010, as this period aligns with the availability of monthly climate data (see below) and ensured minimal loss of TRW data. After cropping the chronologies, their mean values slightly deviated from zero. Therefore, we standardized the chronologies so that their mean values were equal to 1 (Fig. 2, Supplementary Table 2). Subsample signal strength (SSS), a measure of how well a subset of TRW captures the signal present in the entire sample set (Wigley et al., 1984), was calculated according to Cook and Kairiukstis (1992). Only chronologies with an SSS $\geq$0.90 (Supplementary Figure 1) and a length of $\geq$30 annual values within the period

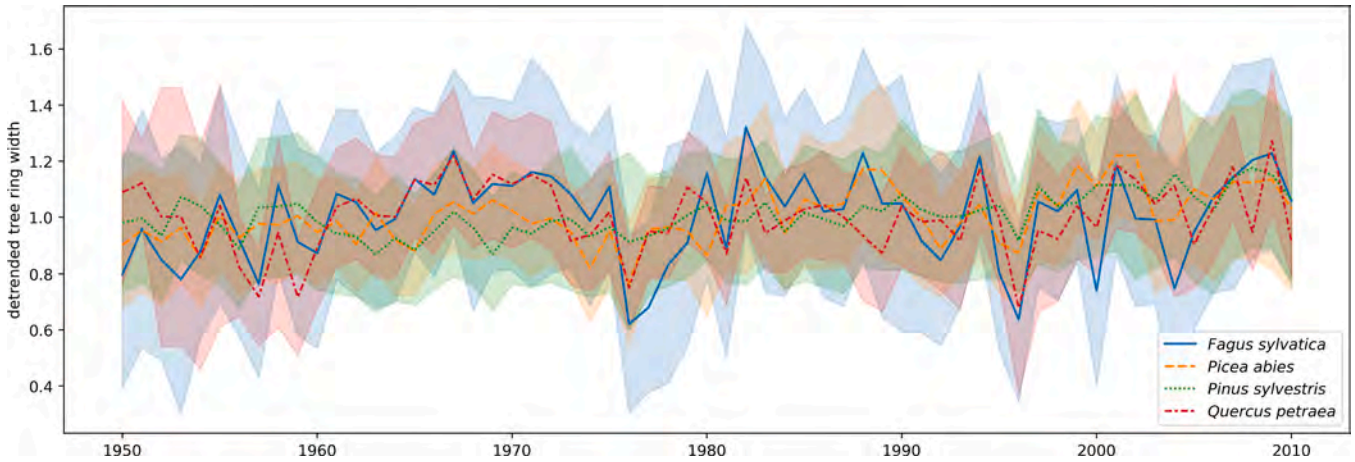


**Fig. 2.** Overview of the selected tree-ring width chronologies in Europe ($TRW_{all}$), derived from the international tree-ring database (ITRDB) and additional tree cores from Austria, used to model the growth of the deciduous broadleaved species *Fagus sylvatica* ($n = 107$), *Quercus petraea* ($n = 40$), and the gymnosperms *Pinus sylvestris* ($n = 319$) and *Picea abies* ($n = 257$) with climate parameters. The lines describe the mean values of 723 age-detrended average chronologies (created using 26,400 trees) in the period 1950 to 2010, with spreads illustrated as shading. See methods for details.

1950–2010 were retained for analysis. Geographical positions for the remaining average were added for each chronology (Fig. 1).

The selected 26,400 tree-ring series were processed and transformed to 723 biweighted-averaged tree-growth chronologies (i.e. the full dataset, $TRW_{all}$, Fig. 2) from 598 sites (Fig. 1, Supplementary Table 1 and Supplementary Table 2), of which 107 were for *F. sylvatica*, 40 for *Q. petraea*, 319 for *P. sylvestris* and 257 for *P. abies*. As weather stations (see below) were available for 236 chronologies (at 179 sites), of which 55 were for *F. sylvatica*, 15 for *Q. petraea*, 42 for *P. sylvestris* and 124 for *P. abies*, the subset $TRW_{AWS}$ was created.

### 2.2. Climatic data

#### 2.2.1. Weather station data

Monthly aggregates, based on daily values, of automatic weather station (AWS) data were obtained for Germany (DWD Climate Data Center, 2021) and Austria (GeoSphere Austria, 2024). For each tree-ring sampling site the nearest AWS was determined. If it was within a radius of 50 km and had a temporal coverage greater than 1960–2005, its data were assigned to the corresponding chronology and included in the $TRW_{AWS}$. Horizontal and vertical differences between sites and adjacent AWS were calculated. Monthly averages of 10 climatic parameters available at all stations, such as (max.) precipitation, extreme and average air temperature, cloud coverage or wind, were used as independent variables (see Supplementary Table 3 for full description). By using the monthly aggregates of the parameters, each parameter resulted in 12 individual independent variables, one per month. To determine their importance for TRW modelling (see below), the AWS-derived parameters/variables were clustered, e.g. 'temperature', which includes all temperature-related parameters/variables (see Supplementary Table 3).

#### 2.2.2. ERA5-Land

The full tree-ring dataset, including 723 chronologies ($TRW_{all}$), as well as the subset of 236 chronologies ($TRW_{AWS}$), were coupled with the ERA5-Land data (C3S, 2019), downloaded using the provided API (CDS, 2024). This dataset has a spatial resolution of 0.1° (~9 km) and an hourly temporal resolution, with coverage from 1950 to the present (C3S, 2024a). We used monthly aggregates (at 2 pm local time) of all available data, except the parameters for "Lakes" and "Invariant" (C3S, 2019), as independent variables (Supplementary Table 4). The monthly averaged reanalysis data by hour of the day consists of two modes: *Accumulated* parameters, which represent the sum of hourly values over the month (e.g., total precipitation), and *instantaneous* parameters, which provide the average value of a parameter (e.g., soil temperature) at a given time of day (i.e. 2 pm). Using 2 pm estimates rather than daily averages (including both day and night) led to slightly improved models (data not shown). The parameter 'wind' as Euclidean distance was calculated using wind along the east-west axis at 10 m height 'u10' and the north-south axis 'v10' (Stull, 2012). ERA5-Land data on leaf area indices (LAI) were not considered as they are given as static parameters (see documentation in C3S (2019)). To compare ERA5-Land derived models with AWS-derived models (see below), the $TRW_{AWS}$ subset was merged with an ERA5-Land data reduced to grid cells matching the available AWS data – creating a separate dataset with equal chronologies. To determine the importance of the parameters for the TRW models (see below), the parameters/variables were clustered according to the categories as provided by ERA5-Land (Supplementary Table 4; (C3S, 2019)).

#### 2.2.3. $CO_2$ and SPEI

The ERA5-Land and AWS datasets were supplemented with monthly *in-situ* $CO_2$ observations from Mauna Loa to integrate the effects of rising atmospheric $CO_2$, anticipated to favour tree growth (Silva et al., 2010). Data on $CO_2$ was retrieved from Keeling at al. (2005), backfilled to 1950, and added as monthly means for each year.

The Standardised Precipitation-Evapotranspiration Index with a temporal 'scale' of 12 months (SPEI12; i.e. current and previous 11 months) was calculated with a rectangular kernel using the R-package 'SPEI' (Beguería and Vicente-Serrano, 2023). SPEI is a water balance index calculated from the monthly difference between precipitation and potential evapotranspiration (PET), with positive values indicating wetness and negative values indicating dryness (Vicente-Serrano et al., 2010). Bhuyan et al. (2017) and Obojes et al. (2024) identified a scale of 12 months (i.e. SPEI12) to best capture the drought responses of European tree species for TRW analyses. Using SPEI of different lengths (e.g., SPEI3, SPEI6) in our dataset did not result in better model performance (data not shown). The input requirements for the calculation of PET were met by the AWS data (Supplementary Table 3), although data gaps occurred. PET was calculated using the Penman-Monteith equation (Monteith, 1965) and gaps in the time series were filled with values calculated according to Hargreaves (1994), which requires less input data. Complete time series of precipitation and PET were provided by the ERA5-Land dataset.

### 2.3. Modelling

We used the linear model Ridge regression (in scikit-learn 'Ridge') with the 'svd' (Singular Value Decomposition) solver. Ridge regression is effective in dealing with multicollinearity by adding L2 regularisation to shrink coefficients (Schreiber-Gregory, 2018), while maintaining a direct interpretability of the model outputs (James et al., 2013). We encountered highly multicollinear independent variables along different axes. For example, soil temperature is highly correlated across different layers (soil depth). In addition, because monthly aggregates were used for each parameter, individual variables were correlated over time, particularly between neighbouring months. By adding penalty to the squared magnitude of coefficients (β), Ridge regression also reduces overfitting. The regularization strength is controlled by the alpha parameter, with higher values increasing the regularization (Pedregosa et al., 2011). Alpha for the AWS-based data regressions was set between 150 and 350 according to previous tests (Supplementary Figure 2).

As the aim was to model the temporal variation of TRW in response to two sources of climate data and to compare the performance, validating the modelling outputs on a temporal scale is reliable (Boser, 2024; Sweet et al., 2023). A 10-fold cross-validation was conducted for each chronology, after all independent variables (see above) were standardised by removing the mean and scaling to unit variance ('StandardScaler') (Pedregosa et al., 2011). The model β for each fold, chronology and dataset were saved and analysed. After grouping β by species, parameter, and month, one-sample *t*-tests ('ttest_1samp') (Virtanen et al., 2020) were applied to assess whether they were significantly different from zero. Models β were aggregated per species and parameter, and sums of absolute values were calculated to quantify the relative 'importance' of each parameter, denoted as 'B'. For illustrative purposes, parameters were grouped into clusters as suggested by C3S (2019).

Predictions made for the $k^{th}$ fold of the cross-validation were evaluated using, linear regressions between actual and predicted values, related coefficients of determination and p-values ('linregress') (Virtanen et al., 2020), and total prediction biases. Mean absolute errors (MAE) were calculated and compared by a *t*-test for paired samples (Virtanen et al., 2020). Kendall's tau (Virtanen et al., 2020) was calculated between residuals and spatial information, i.e. altitudinal and horizontal distances between sites and AWS, and spatial density of AWS (Dahn, 2021).

Detrending and calculation of SPEI12 were done in R (R Core Team, 2024) (version 4.4.2), data processing and analysis were performed using Python 3.12.1, running with IPython 8.23.0, interfaced with Spyder (Raybaut, 2009). Statistical analyses were done using the package Scikit-learn (Pedregosa et al., 2011), and figures were created using matplotlib (Hunter, 2007) and seaborn (Waskom, 2021).

## 3. Results

The full dataset ($TRW_{all}$) consists of 723 averaged tree-growth chronologies from four tree species and 598 sites (Fig. 1). Automatic weather stations (AWS) were available for 236 chronologies, resulting in the subset $TRW_{AWS}$. Climate data from ERA5-Land and AWS were used to model inter-annual changes in tree growth using linear Ridge regression. Model coefficients (or "weights") were captured, with B giving sums of absolute values, to interpret the importance of climatic parameters.

### 3.1. Modelling TRW with weather station data

The drought index SPEI12 was the most important single parameter in the $TRW_{AWS}$ dataset (sum of absolute coefficients B = 0.111), with a consistently positive association with TRW (Fig. 3). Higher values of TRW coincided with higher values of SPEI12 (indicating wetness), particularly in broadleaved species and to a lesser extend in *P. abies*. The parameter sunshine duration ('ssd') was second ranked (B = 0.078) and decreased the TRW of *F. sylvatica* if it occurred in spring, whereas all species gained TRW from more sunshine late in the growing season (September/October). The parameter cloud 'cover' reflected an inverse pattern to 'ssd', with higher cloud cover early in the season having a positive effect on TRW for all species. On third rank, atmospheric $CO_2$ had a consistently positive effect on gymnosperms' TRW. This suggests that $CO_2$ represents a long-term trend in the TRW data (B = 0.061). The importance of parameters is relative to the number of similar parameters within a given cluster – and B of different parameters addressing one driver may in fact accumulate.

The most information by AWS was provided within the cluster air 'Temperature' (Fig. 3, Supplementary Table 5), including five parameters, representing average values and extremes. Higher average air temperature ('t2m' (B = 0.047); and similar averages of 't2m_max' and 't2m_min') promoted tree growth of the gymnosperms, particularly between February and August for *P. sylvestris*, and between March and October for *P. abies* (Fig. 3). In both angiosperms, high average air temperatures early in the growing season (March) were negatively related to TRW. However, within the cluster 'Temperature', monthly extremes ('t2m_max_max' (B = 0.058), 't2m_min_min' (B = 0.050)) were the most important parameters (Fig. 3). For example, high 't2m_max_max' in March and May/June led to a decrease in TRW of *F. sylvatica*. Similar effects were evident for *Q. petraea*. For the gymnosperms *P. sylvestris* and *P. abies*, less extreme 't2m_min_min' in March and subsequent months increased TRW.

Within the cluster 'Wind, pressure and precipitation', parameters on precipitation (B = 0.052–0.055) dominated over wind (B = 0.026); pressure data were not available from AWS (Fig. 3). While monthly accumulated precipitation ('prec') in April to June were related to higher TRW of *F. sylvatica*, high precipitation maxima ('prec_max') in March and July had negative effects. Precipitation effects were less pronounced for *P. sylvestris*, but higher precipitation in February and March increased the stem growth of *P. abies* (Fig. 3).

### 3.2. Modelling TRW with the ERA5-Land dataset

ERA5-Land climate data were applied to the full dataset ($TRW_{all}$) or to a reduced number of chronologies with adjacent AWS (results for the $TRW_{AWS}$ data can be found in Supplementary Figure 3 and Supplementary Table 7). To describe responses on a broader scale, and for the sake of brevity, estimated B for the $TRW_{all}$ dataset are mainly described below, focusing on selected parameters.

Parameters in a model interact with each other, so that the importance of one parameter depends on the values and numbers of other parameters. According to the larger numbers, the parameters in the model based on ERA5-Land data generally had lower weights (Fig. 4) compared to those in the AWS-based model (Fig. 3).

The drought index SPEI12 resulted in largely positive associations with $TRW_{all}$, mainly in spring for *F. sylvatica* and *P. abies*, and during summer for *Q. petraea* and *P. sylvestris*. SPEI12 was thus also the most important single parameter in the ERA5-Land climate dataset; the importance B was 0.085, indicating a relatively stable agreement with TRW. $CO_2$ concentration, as second single most important parameter (B = 0.050), was positively related to tree growth in conifers. The importance of further key individual parameters was similar across clusters, with dew point temperature ('d2m', B = 0.034; i.e. humidity), total precipitation ('tp'; B = 0.033), wind (B = 0.031), surface thermal net radiation ('str' and 'strd'; B = 0.030) and evaporation at the top of the canopy ('evatc'; B = 0.029) having similar importances.

The largest cluster of parameters was 'Evaporation and Runoff', with evaporation at the top of the canopy ('evatc'), sub-surface runoff ('ssro') and evaporation from bare soil ('evabs') as the dominant parameters (B = 0.026–0.029; Fig. 4). The importance of these three parameters was mainly driven by the deciduous species, with high evaporation having a markedly decreasing effect on $TRW_{all}$ except in the late season (September; Fig. 4). However, 'Evaporation and Runoff' parameters were similar and at lower magnitudes for the conifers (Supplementary Table 6). As mentioned above, the total importance of B of akin parameters might add up, likely leading to an underestimation of the total importance of evaporation demands on tree growth.

Sub-surface runoff ('ssro'), a parameter for the total amount of water

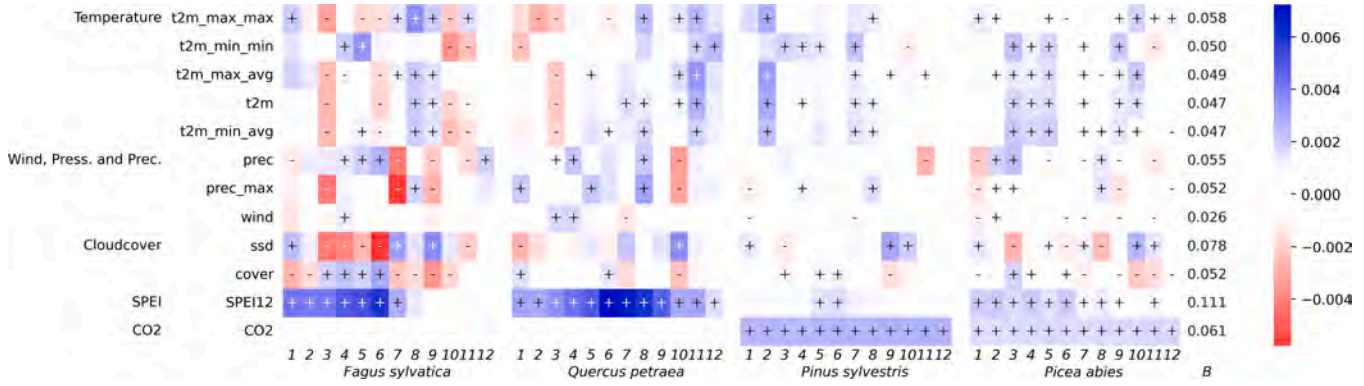


**Fig. 3.** Coefficients (β) of a ridge regression used for modelling tree-ring width of *Fagus sylvatica, Quercus petraea, Pinus sylvestris* and *Picea abies* ($TRW_{AWS}$) against climate data retrieved from nearby weather stations of Austria and Germany, $CO_2$ and SPEI12. The clusters of parameters are listed in descending order according to their importance, defined as $B = \sum|\beta|$ (Supplementary Table 5), while B of each parameter is given on the right. See Supplementary Table 3 for a list of parameters including abbreviations. Averaged β for all tree-ring chronologies are shown coloured, significant differences from zero are labelled with '+' or '-'. Note: an increase in SPEI12 expresses wetter conditions and, thus, a positive correlation reflect an increase in tree growth.

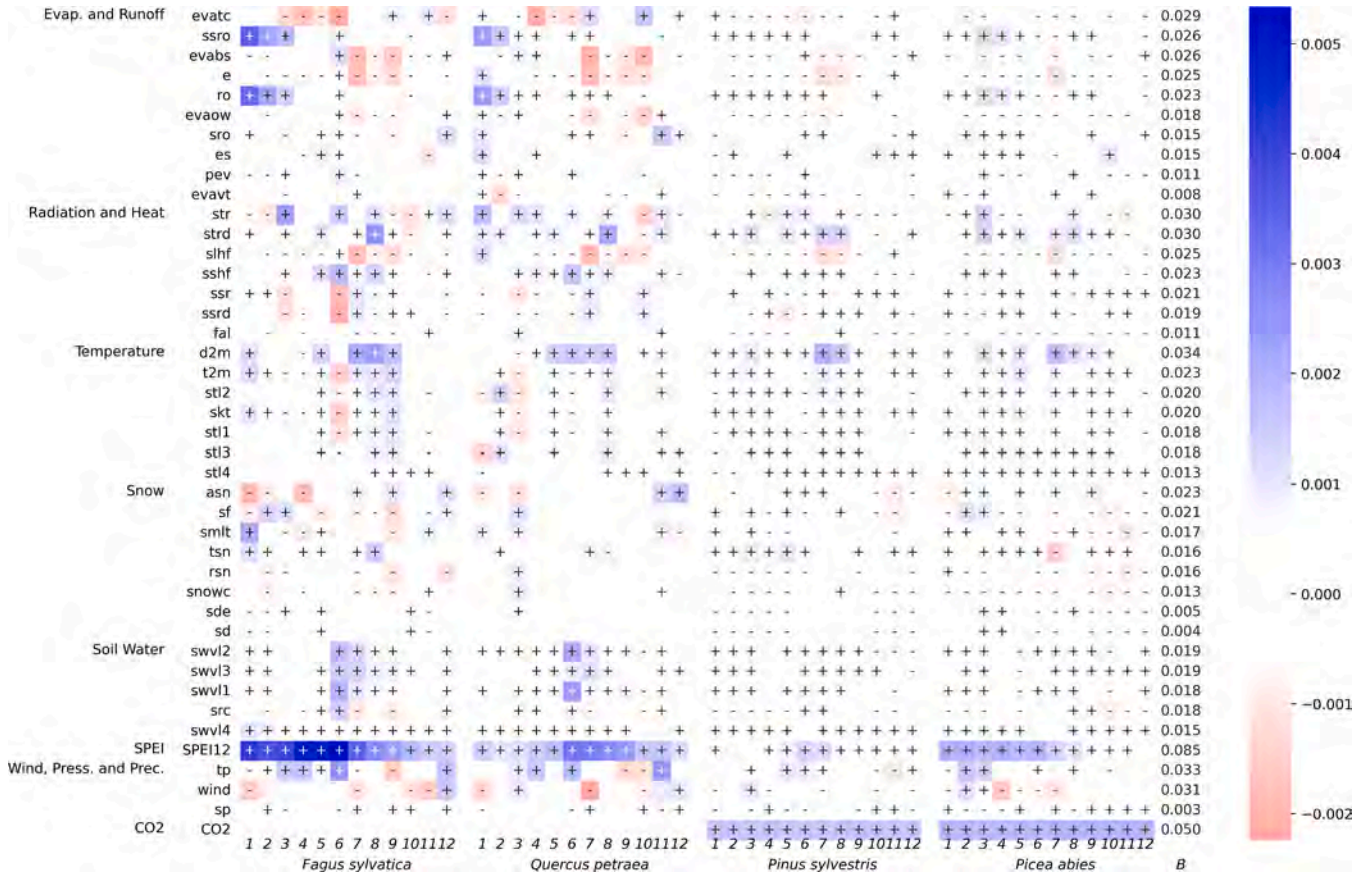


**Fig. 4.** Coefficients (β) of a ridge regression used to model 723 averaged and detrended tree-ring chronologies of four tree species across Europe ($TRW_{all}$), against monthly climate data retrieved from ERA5-Land, $CO_2$ concentration and SPEI12. The clusters of parameters (see Supplementary Table 4) are listed in descending order according to their importance, defined as $B = \sum|\beta|$ (Supplementary Table 6), while B of each parameter is given on the right. Clusters as suggested by C3S (2019). Averaged β for all tree-ring chronologies are shown coloured, significant differences from zero are labelled with '+' or '-'. See Supplementary Figure 3 for the coefficients based on $TRW_{AWS}$ data. Note: an increase in SPEI12 expresses wetter conditions and, thus, a positive correlation reflect an increase in tree growth.

accumulated in the soil, was most important and dominant in January, with its influence diminishing in the following months (Fig. 4). In *F. sylvatica* and *Q. petraea*, the parameters 'ssro' and 'ro' (both parameters on soil water availability, Supplementary Table 4) clearly decreased in importance as volumetric soil water content ('swvl1 to 3') gained significance. Within the 'Soil Water' cluster, moisture estimates for layer 2 ('swvl2'; i.e. 7–28 cm) showed to be most important (Fig. 4). The summer month from June onwards turned out to be the most important months for the deciduous species. Similar patterns of β were observed for the coniferous species, however, also soil moisture estimates in January and February had a considerable impact on TRW. The magnitude of B was substantially lower for gymnosperms (Supplementary Table 6), due to their wide spatial distribution across Europe (Fig. 1), as the range of B was higher for the subset $TRW_{AWS}$ at Austrian and German sites (Supplementary Figure 3, Supplementary Table 7).

Besides soil moisture, soil temperature is the second key set of parameters that provide information about soils. Estimates for layer 2 ('stl2') showed to be the most important ones as compared to other soil depths (Fig. 4). More important than soil temperature ($B$ = 0.018–0.020), however, were air and dew point temperatures, showing varying effects on TRW depending on the species (Supplementary Table 6). In specific, dewpoint temperature ('d2m'; B = 0.034), a measure of air humidity, showed largely positive effects for all species during spring and summer. Average air temperature ('t2m') was of lesser importance ($B$ = 0.023). For all species except *P. abies*, high ranges of air, surface ('skt') and topsoil temperatures in June negatively affected TRW. *Q. petraea* showed to be sensible to higher temperatures in March.

An additional driver for TRW of *Q. petraea* was given by snow albedo 'asn', i.e. the reflectivity of the snow-covered land in March, was an additional driver of TRW for *Q. petraea*. Similar effects of 'asn' until early spring were found for *F. sylvatica*. Across species, 'asn' ($B$ = 0.023) was inconsistent with strong negative relationships with TRW in deciduous trees in March/April (i.e. late snow) and positive relationships with remaining snow during the growing season, possibly at higher altitudes/latitudes, providing a water source for *P. abies*.

Finally, within the 'Wind, Pressure and Precipitation' cluster, total precipitation ('tp') dominated ($B$ = 0.033), with rainfall early in the growing season benefiting tree-ring growth in all species, but to a significantly greater extent in *F. sylvatica*.

### 3.3. Prediction of detrended TRW and residual analysis

The AWS-based data allowed models to be trained for 236 chronologies, but only 227 chronologies could be used for validation due to gaps in the meteorological data. TRW predictions for this dataset were correlated with actual values, with an $R^2$ of 0.15 ($p < 0.001$) across species. When using ERA5-Land data and corresponding derivatives for the same chronologies, correlations between actual and predicted values reached similar quality ($R^2$ = 0.13). The only marked differences in species-specific model quality between AWS and ERA5-Land based models were found for *Q. petraea*, with an $R^2$ of 0.07 for AWS and $R^2$ of 0.02 for ERA5-Land (at AWS; Fig. 5). However, *Q. petraea* was represented by the fewest number of sites ($n$ = 15) compared to the other three species ($n$ = 42–119 sites).

Due to the consistent and global coverage by ERA5-Land data, all 723 chronologies across Europe could be modelled and validated using

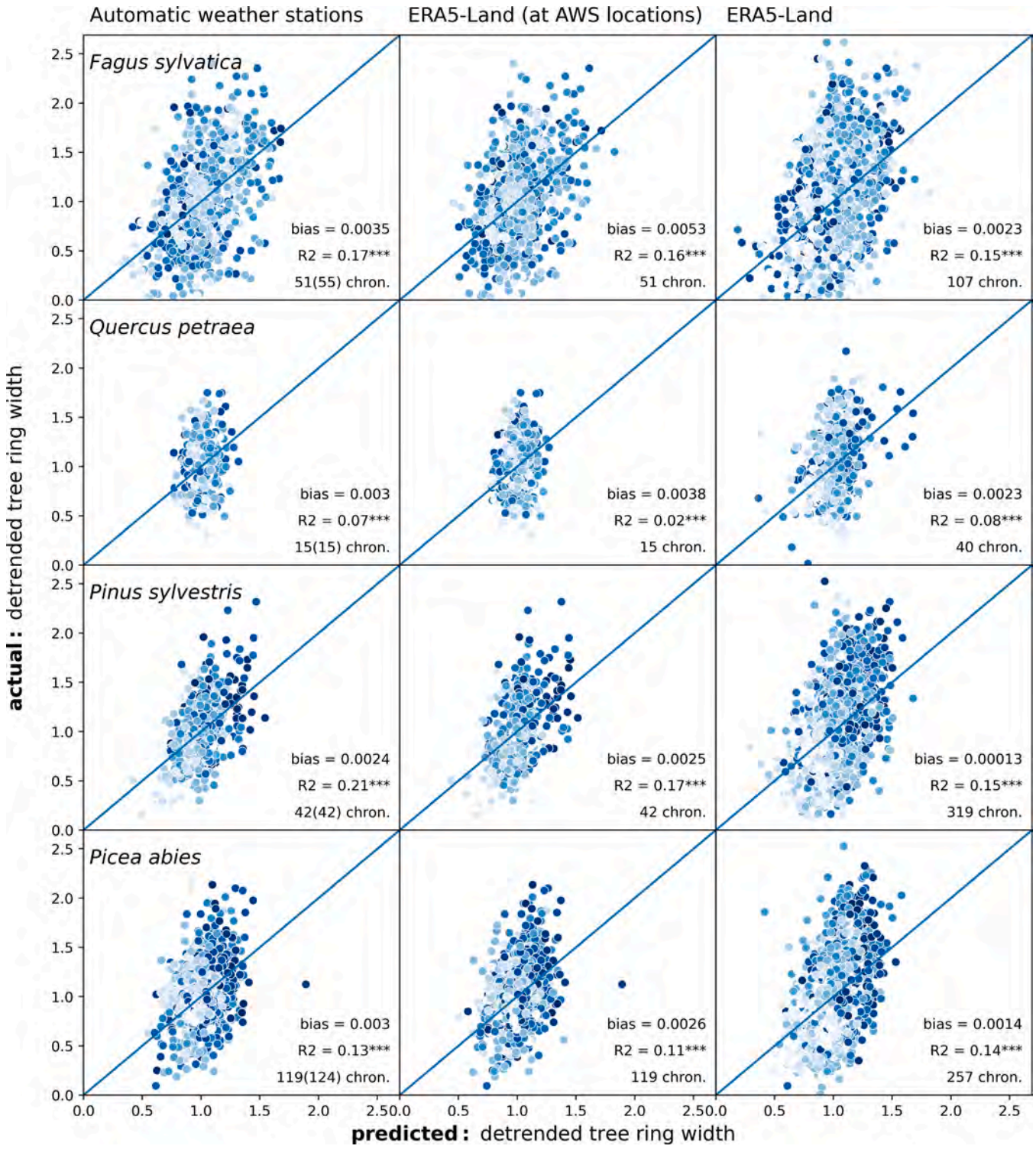


**Fig. 5.** Predictions of the detrended tree-ring width (TRW) of four European tree species made during a 10-fold cross validation. Models are based on a subset of sites related to automatic weather stations (AWS; left column) and a matched subset of ERA5-Land data (middle; $TRW_{AWS}$), or the climate data from the ERA5-Land dataset for all available chronologies (right; $TRW_{all}$). The total bias of predictions, coefficients of determination ($R^2$), and the number of chronologies within the test set (number of total chron. in brackets) are given. Asterisks indicate levels of significance, *** $p < 0.001$, ** $p < 0.01$, * $p < 0.05$.

$TRW_{all}$. Similar to the subset $TRW_{AWS}$, predicted values corresponded well to actual values in $TRW_{all}$, with an $R^2$ of 0.15 ($p < 0.001$) across species. Again, model performance was similar for all species between AWS and the full ERA5-Land set of TRW, but improved for *Q. petraea* in $TRW_{all}$ to the level of AWS, possibly due to the increased number of chronologies ($n = 40$). Prediction models for *P. abies* also benefited slightly from using the full European dataset ($R^2 = 0.14$). Highly significant correlations were found for all datasets.

Residuals were calculated for the 236 chronologies covered by both the AWS data and the ERA5-Land dataset (i.e. $TRW_{AWS}$). The mean absolute error (MAE) for the AWS-based analysis was 0.18 (±0.09 standard deviation). Comparison of the MAE with altitude differences

between the spatial origin of the chronologies and adjacent AWS revealed no significant correlation (Fig. 6B). The horizontal distance to the nearest AWS showed a negative influence on the MAE, meaning that proximate weather stations resulted in higher biases, probably caused by a few conspicuously high MAE values (≥0.45; Fig. 6B). The MAE of the predictions using the corresponding ERA5-Land dataset resulted in similar residuals (0.18±0.09) compared to AWS ($p = 0.07$, Fig. 6A). Although the spatial density of AWS varied substantially over the subset of experimental area (Fig. 6C), high densities of AWS did not reduce the mean absolute error (MAE) in our study (Fig. 6D). In fact, a weak increase in MAE was observed with higher densities of AWS ($p = 0.03$ and $p = 0.01$, for AWS and ERA5-Land based models).

## 4. Discussion

Modelling the relationship between annual tree-ring width (TRW) and climate parameters is essential for our understanding of ecological responses in a plant-atmosphere continuum and plant functioning (Anderegg et al., 2015; Babst et al., 2019). Until now, it has been unclear whether (1.) ERA5-Land parameters, with their high spatial resolution and long temporal coverage, can replace meteorological data from weather stations for modelling TRW in Europe, and (2.) if the extended climate parameter set of ERA5-Land has the potential to improve our mechanistic understanding of species-specific growth responses.

### 4.1. Modelling tree-ring width using meteorological or ERA5-Land climate data

The modelling of tree-ring chronologies across Europe ($TRW_{all}$) with ERA5-Land parameters produced predictions with reliable associations to actual values, with an $R^2$ of 0.15. Comparisons of model performance with previous research are challenging due to the diverse approaches in modelling, used dependent and independent variables, output validation, and reporting of prediction quality. For instance, Martínez-Fernández et al. (2019) examined the applicability of remote sensing products for modelling TRW data from 1978 to 2016 of 22 pine stands in Spain, identifying clear temporal interrelations with satellite-based estimates for soil moisture. However, their study did not validate predictions on an independent test dataset. Jevšenak et al. (2024) developed species-specific spatio-temporal models to predict raw

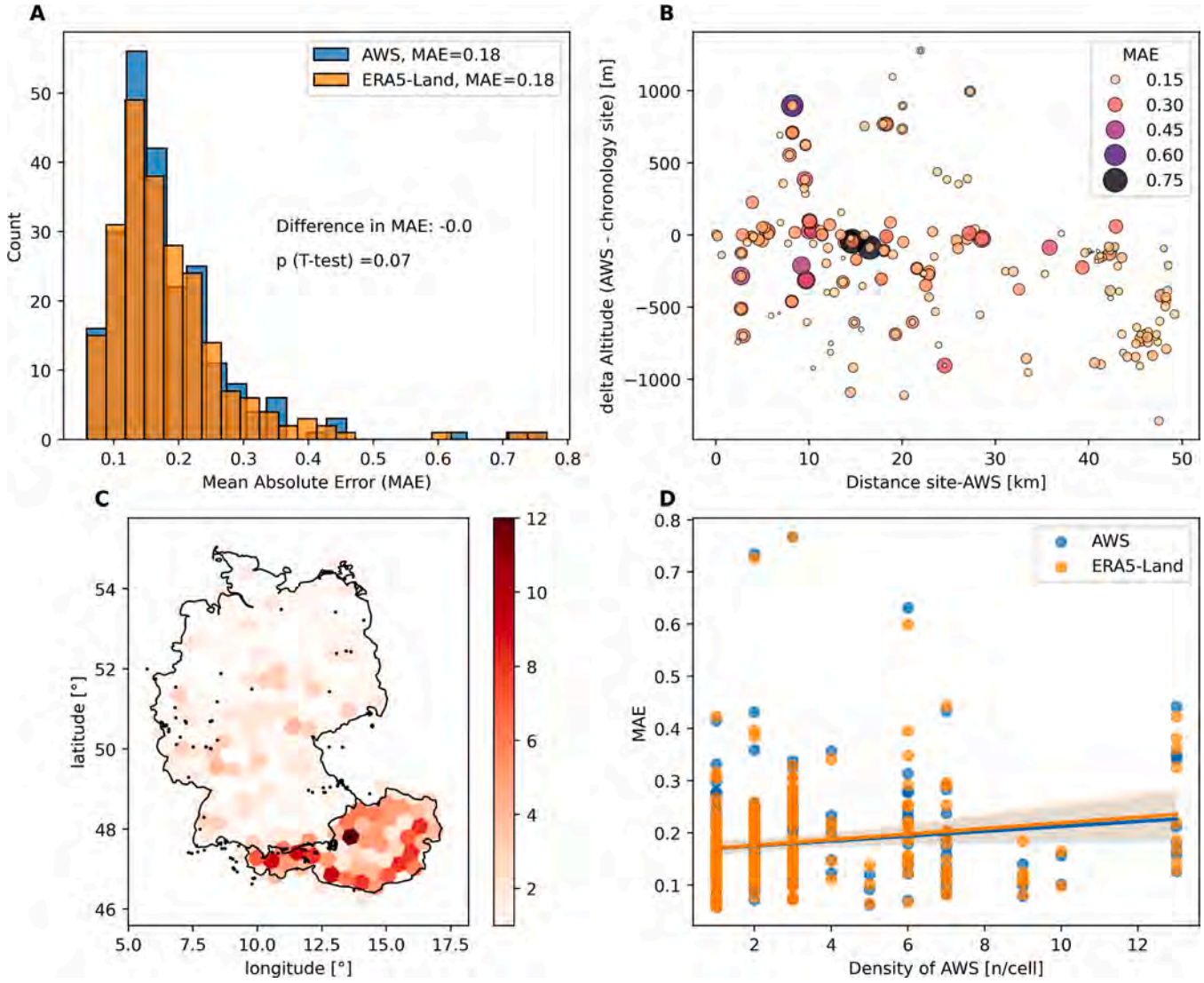


**Fig. 6.** Mean average error (MAE) of the predictions for models based on the AWS and ERA5-Land datasets, respectively (A), with its dependence of errors on differences in altitude (m) and horizontal distance (km) between the weather station (AWS) and $TRW_{AWS}$ site / tree stand (B). Subplot (C) illustrates the density of AWS (heatmap) and the positions of tree ring chronologies (dots). MAE for predictions of $TRW_{ERA}$ slightly increased with density of stations (C), but similar to the distribution of MAE within the $TRW_{AWS}$ data.

TRW values (since 2018) using vegetation indices, topography, and climate data across Europe. Using blocked k-fold cross validation, their models achieved an overall $R^2$ of 0.13, peaking at 0.52 for *Q. petraea*. Predicting raw values, also done using forward-modelling by Breitenmoser et al. (2014), tend to have higher variability in inferred correlations (Ols et al., 2023), making comparisons with our study difficult. Similarly, raw tree-ring width values from 62 Sierra Nevada sites showed that legacy effects, as reflected in MODIS GPP estimates, effectively described tree growth of dominant evergreen species (Wong et al., 2021). Although global or large-scale datasets have already been used to model long time series of TRW (e.g. Manvailer and Hamann, 2024; Wang et al., 2024), previous work tended to focus on selected parameters, whereas a broad spectrum of information is available from ERA5-Land.

In total, the modelling outputs were similar between the two sources of climate data. Mean absolute error was ±0.18 using ERA5-Land data and ±0.18 with AWS-based data, confirming the suitability of ERA5-Land data for TRW modelling compared to meteorological AWS data. The similarity in predictive quality can be explained by the relatedness of ERA5-Land and AWS data. In fact, the ERA5-Land assimilation is a downscaled version of the ERA5 climate reanalysis (Muñoz-Sabater et al., 2021), which is based on satellite data and *in-situ* observations partly derived from weather stations (C3S, 2024a). A good global agreement with *in-situ* measurements has been confirmed for ERA5-Land parameters, e.g. precipitation (Manvailer and Hamann, 2024). Due to the rather coarse grid cell sizes of ERA5 (~31 × 31 km) and ERA5-Land (~9 × 9 km), detailed site-specific information, such as topography and related climatic aspects are ignored. This may reduce the impact of high densities of in-situ data within individual ERA5 grid cells. Consistent with this, we did not observe a positive effect of high AWS granularity on prediction errors (Fig. 6D). When using the AWS data from nearest stations (radius ≤ 50 km) high quality information on e.g. precipitation and temperature is considered. Also, the altitude of the site was integrated for calculating SPEI time series of the respective chronologies when using the AWS dataset for modelling. Distinct elevational responses determine tree growth in combination with temperature regimes (Paulsen et al., 2000) – which might have contributed to the performance of AWS-based analysis. In our study, the distance between the site and AWS, as well as altitudinal differences, did, however, not increase MAE, as predictions with high errors appeared to be randomly distributed across the geographic differences (Fig. 6).

Whereas adjacent AWS are thus a reliable source for high quality meteorological data, they usually lack extensive spatiotemporal coverage (Fig. 6C, Capra et al., 2013; Castellanos-Acuna and Hamann, 2020) and are prone to data gaps and exhibit varying coverage of parameters (WMO, 2023). The overlap of commonly measured (i.e. core) parameters between countries can be small. As a result, only 10 meteorological parameters from weather stations and 227 out of the AWS subset consisting of 236 chronologies could be used for modelling. Moreover, data from AWS are often only accessible through national agencies with limited availability (Pelosi et al., 2021). When modelling tree growth in regions not covered by synchronized repositories (e.g. Horel and Dong, 2010; Klein Tank et al., 2002), the compilation and integration of meteorological data at large scales becomes almost infeasible, or at best very labour intensive. In contrast, the ERA5-Land dataset is comprehensive, openly available (C3S, 2019; CDS, 2024; Hufkens, 2019), and designed to be applicable, interoperable, and ready-to-use. Still, these data is never free from uncertainties due to grid-to-point transfer, scale mismatches and representativeness issues (Amjad et al., 2020).

### 4.2. Climate parameters critical to (future) tree growth modelling

Our data indicates that the drought index SPEI12 has had a strong effect on age-detrended and site-averaged ring width of tree species across Europe. The index thereby showed once more its predictive power for tree growth (Thom et al., 2023). The consistent monthly pattern observed across species evidence that the SPEI is of similar high quality when calculated based on either AWS or ERA5-Land data. The general good coupling is probably because the SPEI uses the difference between precipitation and potential evapotranspiration and thereby incorporates the effects of global warming more directly – increasing its applicability beyond indices based on precipitation alone (e.g. SPI) (Nwayor and Robeson, 2024). The 12-month scale integrates longer-term drought legacies and ecosystem water balances and has previously been shown to be particularly suited for TRW modelling (Bhuyan et al., 2017; Obojes et al., 2024). The legacy effects of previous growth conditions can be partly attributed to the lifespan of functional organs and the storage of carbon reserves, with tree species with longer organ and reserve lifespans tending to be characterized by stronger legacy effects (Zweifel and Sterck, 2018). While it has been reported that European conifers are more susceptible to extreme droughts than broadleaves (Thom et al., 2023), our data indicates that the gymnosperms also profit less from preceding wetter conditions than broadleaves – for which the SPEI12 pattern indicate a stronger positive correlation of longer-term water supply to tree-ring growth. We can only speculate that the diverging response may be related to differences in hydraulic systems and other traits between broadleaves and gymnosperms. However, it is important to note that the SPEI12 calculated here integrates different legacy signatures within an annual scale, e.g. dry summers followed by 'average' springs, wet winters followed by 'average' summers, and also averages responses across bioclimatic regions. Wu et al. (2022) have previously shown that the importance and magnitude of legacy effects relative to current water deficit varies considerably depending on the temporal occurrence of seasonal climate extremes, urging to identify specific climate scenarios (within bioclimatic regions) for a more detailed analyses of TRW effects in the future.

Apart from parameters related to ERA5-Land or AWS, carbon dioxide concentration has had a strong and consistently positive effect on TRW of both studied gymnosperms across Europe; these $CO_2$ effects were consistent in magnitude and importance (i.e. 2nd or 3rd single most important parameter) in both ERA5-Land and AWS-based models. Whereas experimental studies on younger stands already showed two decades ago that elevated $CO_2$ can increase net primary productivity (Norby et al., 2005), uncertainties remained as to whether these effects scale to mature forests due to disturbance, N deposition/limitation and/or climate change induced drought (e.g. Gedalof and Berg, 2010). However, Davis et al. (2022) recently showed that $CO_2$ fertilisation effects are widespread in North American forests, with the strongest effects in forests dominated by *Pinus* spp. and *Picea* spp. in agreement with our results. The contrast between angiosperms and gymnosperms is likely to be due to fundamental physiological differences, as modulated by $O_2$:$CO_2$ ratios, vapour pressure deficit, and/or temperature (Hare and Lavergne, 2021).

In addition to the calculated SPEI and atmospheric $CO_2$, the 'standard' meteorological parameters available in both datasets, such as air temperature ('t2m'), monthly precipitation ('tp' in ERA5-Land and 'prec' in AWS, respectively), or those related to radiation (e.g. 'str'/'strd' or 'ssd', respectively), are, as expected, of key importance in both models (e.g. Leuchner et al., 2012; Way and Oren, 2010). However, the importance of these parameters for tree growth varies not only between species, as shown, but also between biogeoclimatic regions, with an expected interaction of geographical variables (latitude or altitude) with precipitation and/or temperature (Babst et al., 2013). Similarly, the intensity and length of the photoperiod determines the seasonality of tree processes including xylogenesis and thus the amount of growth (Way and Montgomery, 2015) yet it is closely correlated with latitude. While our data thus confirms the general suitability of ERA5-Land data to substitute corresponding AWS parameters, an in-depth ecological interpretation requires an improved spatial representation beyond the scope of this study.

In addition to the convenient and consistent availability of these core

parameters, we argue that a major advantage of ERA5-Land is the immediate availability of less frequently used parameters. Air humidity (represented by 'd2m') was found to be an important parameter in the ERA5-Land model across all four species and seasons, confirming recent results of experimental studies for selected species (Güney et al., 2020; Oogathoo et al., 2024) while being only available for selected AWS. Furthermore, dendroclimatology has mainly focused on the response of TRW to atmospheric variables, whereas roots sense the 'subsurface climate', which has been reported to be equally important for tree growth (Belokopytova et al., 2021; Kostić et al., 2021). Direct measurements of soil-related parameters are not standard among AWS and rarely represent forest soils. The ERA5-Land dataset has been shown to be in alignment with *in-situ* measurements for soil temperature (Gomis-Cebolla et al., 2023; Zhang et al., 2024) and soil moisture (Lal et al., 2022; Xing et al., 2023; Schönauer et al., 2025). In our data set, soil moisture and temperature estimates at a depth of 7–28 cm, i.e. the main rooting zone, had the most considerable impact on TRW. Our results also indicated that low spring temperatures and the associated snow cover negatively affected the growth of both *Fagus sylvatica* and *Quercus petraea*. At the onset of the growing season, cambial activity is initiated shortly after snowmelt, driven by the relevance of snow cover for soil moisture and temperature (Sanmiguel-Vallelado et al., 2021), suggesting that snow cover, particularly before and during the early growing season, may be an important future parameter in dendrochronology (Sanmiguel-Vallelado et al., 2021; Vaganov et al., 1999). As a final 'belowground' example, an increased winter water storage, represented by the 'runoff' parameters, showed a clear effect on the TRW of all species, especially the two angiosperms. Although rising temperatures and changing precipitation regimes may prolong winter droughts, winter water storage has not been integrated into common tree growth models (Ashraf et al., 2015; Gupta and Sharma, 2019; Härkönen et al., 2019), but may become increasingly important in the future as data availability improves (Roderick et al., 2015).

Recent and ongoing advances in Earth observation satellites continue to increase the availability of diverse spatio-temporal data on land and atmospheric conditions (Bauer-Marschallinger et al., 2019; Das et al., 2020; Quast et al., 2023), thereby expanding their potential to refine traditional growth models. As the length of periods with suitable conditions determines annual growth (Etzold et al., 2022), the high temporal resolution available for ERA5-Land bears further advantages. The plethora of parameters covered by global data products could thus replace conventional input data and their derivatives, further improving the predictive power of tree growth models used for an era of climate change (Babst et al., 2019).

### 4.3. Conclusion and outlook

Understanding vegetation-climate interactions through dendrochronological studies is critical for predicting future ecosystem responses to global change. This study demonstrates that the ERA5-Land dataset can be used to successfully model the tree-ring width (TRW) of four common tree species across Europe. The model performance achieved, comparable to the use of meteorological data from nearby weather stations, highlights the potential of ERA5-Land as a valuable resource for dendrochronological studies worldwide. In addition, unlike data from weather stations, ERA5-Land is openly accessible, easy to use, provides global coverage since 1950 and includes a variety of standardized environmental parameters above and below ground. These facilitate in-depth analysis of environment-vegetation interactions and will help to improve our understanding of growth responses to less commonly studied environmental changes, such as humidity, soil moisture and snow cover. Looking ahead, we encourage the wider use of ERA5-Land data to improve tree growth models, particularly for assessing long-term climate-growth relationships and reducing predictive uncertainties. We call for further refinement of ERA5-Land data by accounting for altitude within smaller grid cells and yearly vegetation parameters. Future studies should explore the potential of integrating additional reanalysis products, remote sensing data, and physiological modelling approaches to further enhance prediction accuracy. By advancing our understanding of tree-climate interactions, we can develop more robust frameworks for forest conservation, carbon sequestration, and climate adaptation, ultimately supporting natural forest dynamics and sustainable ecosystem management in a rapidly changing world.

## CRediT authorship contribution statement

**Marian Schönauer:** Writing – review & editing, Writing – original draft, Visualization, Validation, Methodology, Investigation, Funding acquisition, Formal analysis, Data curation, Conceptualization. **Christoph Pucher:** Writing – review & editing, Writing – original draft, Visualization, Validation. **Jan Altman:** Writing – review & editing, Writing – original draft, Validation. **Josef Weißbacher:** Writing – review & editing, Data curation. **Lars Sprengel:** Writing – review & editing, Data curation. **Boris Rewald:** Writing – review & editing, Writing – original draft, Validation.

## Declaration of competing interest

The authors declare that they have no known competing financial interests or personal relationships that could have appeared to influence the work reported in this paper.

## Acknowledgments

We want to thank Marius Möller for conducting tree-ring width measurements. MS received financial support by the Eva Mayr-Stihl Stiftung for the analysis of tree cores. MS and BR were funded by the European Union under Horizon Europe (project EXCELLENTIA, GA No 101087262) during the data analyses and manuscript preparation stage. JA was supported by the Czech Science Foundation (23–07533S), the long-term research development project No RVO 67985939 of the Czech Academy of Sciences, and Estonian Research Council (grant PSG1044). We thank two anonymous reviewers for their helpful comments on an earlier version of the manuscript.

## Supplementary materials

Supplementary material associated with this article can be found, in the online version, at doi:10.1016/j.agrformet.2025.110679.

## Data availability

The datasets generated during and/or analysed during the current study are available in the Zenodo repository, https://doi.org/10.5281/zenodo.15592062. Model codes are available on GitHub, https://github.com/marianschoenauer/TreeRingWidth.git.

## References

Altman, J., Hédl, R., Szabó, P., Mazůrek, P., Riedl, V., Müllerová, J., Kopecký, M., Doležal, J., 2013. Tree-rings mirror management legacy: dramatic response of standard oaks to past coppicing in Central Europe. PLoS ONE 8, e55770. https://doi.org/10.1371/journal.pone.0055770.

Amjad, M., Yilmaz, M.T., Yucel, I., Yilmaz, K.K., 2020. Performance evaluation of satellite- and model-based precipitation products over varying climate and complex topography. J. Hydrol. 584, 124707. https://doi.org/10.1016/j.jhydrol.2020.124707.

Anderegg, W.R.L., Schwalm, C., Biondi, F., Camarero, J.J., Koch, G., Litvak, M., Ogle, K., Shaw, J.D., Shevliakova, E., Williams, A.P., Wolf, A., Ziaco, E., Pacala, S., 2015. Pervasive drought legacies in forest ecosystems and their implications for carbon cycle models. Science 349, 528–532. https://doi.org/10.1126/science.aab1833.

Arco Molina, J.G., Saurer, M., Altmanova, N., Treydte, K., Dolezal, J., Song, J.-S., Altman, J., 2024. Recent warming and increasing $CO_2$ stimulate growth of dominant

trees under no water limitation in South Korea. Tree Physiol 44. https://doi.org/10.1093/treephys/tpae103 tpae103.
Ashraf, M.I., Meng, F.-R., Bourque, C.P.-A., MacLean, D.A., 2015. A novel modelling approach for predicting forest growth and yield under climate change. PLOS ONE 10, e0132066. https://doi.org/10.1371/journal.pone.0132066.
Babst, F., Poulter, B., Trouet, V., Tan, K., Neuwirth, B., Wilson, R., Carrer, M., Grabner, M., Tegel, W., Levanic, T., Panayotov, M., Urbinati, C., Bouriaud, O., Ciais, P., Frank, D., 2013. Site- and species-specific responses of forest growth to climate across the European continent: climate sensitivity of forest growth across Europe. Glob. Ecol. Biogeogr. 22, 706–717. https://doi.org/10.1111/geb.12023.
Babst, F., Bouriaud, O., Poulter, B., Trouet, V., Girardin, M.P., Frank, D.C., 2019. Twentieth century redistribution in climatic drivers of global tree growth. Sci. Adv. 5, eaat4313. https://doi.org/10.1126/sciadv.aat4313.
Balting, D.F., AghaKouchak, A., Lohmann, G., Ionita, M., 2021. Northern Hemisphere drought risk in a warming climate. Npj Clim. Atmospheric Sci. 4, 61. https://doi.org/10.1038/s41612-021-00218-2.
Bauer-Marschallinger, B., Freeman, V., Cao, S., Paulik, C., Schaufler, S., Stachl, T., Modanesi, S., Massari, C., Ciabatta, L., Brocca, L., Wagner, W., 2019. Toward global soil moisture monitoring with Sentinel-1: harnessing assets and overcoming obstacles. IEEE Trans. Geosci. Remote Sens. 57, 520–539. https://doi.org/10.1109/TGRS.2018.2858004.
Beguería, S., Vicente-Serrano, S.M.. SPEI: calculation of the standardized precipitation-evapotranspiration Index. https://github.com/sbegueria/SPEI.
Belokopytova, L.V., Zhirnova, D.F., Meko, D.M., Babushkina, E.A., Vaganov, E.A., Krutovsky, K.V., 2021. Tree rings reveal the impact of soil temperature on larch growth in the forest-steppe of Siberia. Forests 12, 1765. https://doi.org/10.3390/f12121765.
Berg, A., Sheffield, J., 2018. Climate Change and drought: the soil moisture perspective. Curr. Clim. Change Rep. 4, 180–191. https://doi.org/10.1007/s40641-018-0095-0.
Berry, P.A.M., Smith, R., Benveniste, J., 2018. Altimeter Corrected Elevations, version 2 (ACE2). https://doi.org/10.7927/H40G3H78.
Bhuyan, U., Zang, C., Menzel, A., 2017. Different responses of multispecies tree ring growth to various drought indices across Europe. Dendrochronologia 44, 1–8. https://doi.org/10.1016/j.dendro.2017.02.002.
Bitterlich, W., 1952. Die winkelzählprobe: ein optisches meßverfahren zur raschen aufnahme besonders gearteter probeflächen für die bestimmung der Kreisflächen pro hektar an stehenden Waldbeständen. Forstwiss. Cent. 71, 215–225. https://doi.org/10.1007/BF01821439.
Blanco, J.A., Lo, Y.-H., 2023. Latest trends in modelling forest ecosystems: new approaches or just new methods? Curr. For. Rep. 9, 219–229. https://doi.org/10.1007/s40725-023-00189-y.
Bose, A.K., Doležal, J., Scherrer, D., Altman, J., Ziche, D., Martínez-Sancho, E., Bigler, C., Bolte, A., Colangelo, M., Dorado-Liñán, I., Drobyshev, I., Etzold, S., Fonti, P., Gessler, A., Kolář, T., Koňasová, E., Korznikov, K.A., Lebourgeois, F., Lucas-Borja, M. E., Menzel, A., Neuwirth, B., Nicolas, M., Omelko, A.M., Pederson, N., Petritan, A.M., Rigling, A., Rybníček, M., Scharnweber, T., Schröder, J., Silla, F., Sochová, I., Sohar, K., Ukhvatkina, O.N., Vozmishcheva, A.S., Zweifel, R., Camarero, J.J., 2024. Revealing legacy effects of extreme droughts on tree growth of oaks across the Northern Hemisphere. Sci. Total Environ. 926, 172049. https://doi.org/10.1016/j.scitotenv.2024.172049.
Boser, A., 2024. Validating spatio-temporal environmental machine learning models: simpson's paradox and data splits. Environ. Res. Commun. 6, 031003. https://doi.org/10.1088/2515-7620/ad2e44.
Breitenmoser, P., Brönnimann, S., Frank, D., 2014. Forward modelling of tree-ring width and comparison with a global network of tree-ring chronologies. Clim. Past 10, 437–449. https://doi.org/10.5194/cp-10-437-2014.
Bugmann, H., 2001. A review of forest gap models. Clim. Change 51, 259–305. https://doi.org/10.1023/A:1012525626267.
Bunn, A., Korpela, M., Biondi, F., Campelo, F., Mérian, P., Qeadan, F., Zang, C., 2024. dplR: dendrochronology Program Library in R.
Bunn, A.G., 2008. A dendrochronology program library in R (dplR). Dendrochronologia 26, 115–124. https://doi.org/10.1016/j.dendro.2008.01.002.
Bunn, A.G., 2010. Statistical and visual crossdating in R using the dplR library. Dendrochronologia 28, 251–258. https://doi.org/10.1016/j.dendro.2009.12.001.
C3S, - Copernicus Climate Change Service, 2019. ERA5-Land monthly averaged data from 1950 to present. https://doi.org/10.24381/CDS.68D2BB30.
C3S, - Copernicus Climate Change Service, 2024. The family of ERA5 datasets, https://confluence.ecmwf.int/display/CKB/The+family+of+ERA5+datasets.
Capra, A., Consoli, S., Scicolone, B., 2013. Long-term climatic variability in Calabria and effects on drought and agrometeorological parameters. Water Resour. Manag. 27, 601–617. https://doi.org/10.1007/s11269-012-0204-0.
Castellanos-Acuna, D., Hamann, A., 2020. A cross-checked global monthly weather station database for precipitation covering the period 1901–2010. Geosci. Data J. 7, 27–37. https://doi.org/10.1002/gdj3.88.
CDS, 2024. How to install and use CDS API on Windows. Climate Data Store.
Cook, E.R., Kairiukstis, L.A., 1992. Methods of dendrochronology: applications in the environmental sciences. Repr. d. Ausg. 1990. International Institute for Applied Systems Analysis, Dordrecht u. a.
Dahn, 2021. H3-Pandas.
Das, N., Entekhabi, D., Dunbar, R., Kim, S., Yueh, S., Colliander, A., ONeill, P., Jackson, T., Jagdhuber, T., Chen, F., Crow, W., Walker, J., Berg, A., Bosch, D., Caldwell, T., Cosh, M., 2020. SMAP/sentinel-1 L2 radiometer/radar 30-second scene 3 km EASE-grid soil moisture, version 3. https://doi.org/10.5067/ASB0EQO2LYJV.
Davis, E.C., Sohngen, B., Lewis, D.J., 2022. The effect of carbon fertilization on naturally regenerated and planted US forests. Nat. Commun. 13, 5490. https://doi.org/10.1038/s41467-022-33196-x.
DWD Climate Data Center, 2021. Historische tägliche Stationsbeobachtungen (Temperatur, Druck, Niederschlag, Sonnenscheindauer, etc.) für Deutschland: version v21.3.
Etzold, S., Waldner, P., Thimonier, A., Schmitt, M., Dobbertin, M., 2014. Tree growth in Swiss forests between 1995 and 2010 in relation to climate and stand conditions: recent disturbances matter. For. Ecol. Manag. 311, 41–55. https://doi.org/10.1016/j.foreco.2013.05.040.
Etzold, S., Sterck, F., Bose, A.K., Braun, S., Buchmann, N., Eugster, W., Gessler, A., Kahmen, A., Peters, R.L., Vitasse, Y., Walthert, L., Ziemińska, K., Zweifel, R., 2022. Number of growth days and not length of the growth period determines radial stem growth of temperate trees. Ecol. Lett. 25, 427–439. https://doi.org/10.1111/ele.13933.
FOREST EUROPE., 2020. State of Europe's forests 2020. Bratislava, Slovak Republic.
Güney, A., Zweifel, R., Türkan, S., Zimmermann, R., Wachendorf, M., Güney, C.O., 2020. Drought responses and their effects on radial stem growth of two co-occurring conifer species in the Mediterranean mountain range. Ann. For. Sci. 77, 105. https://doi.org/10.1007/s13595-020-01007-2.
Gedalof, Z., Berg, A.A., 2010. Tree ring evidence for limited direct $CO_2$ fertilization of forests over the 20th century. Glob. Biogeochem. Cycles 24. https://doi.org/10.1029/2009GB003699, 2009GB003699.
GeoSphere Austria, 2024. Messstationen monatsdaten v2. https://doi.org/10.60669/923N-P390.
Gomis-Cebolla, J., Rattayova, V., Salazar-Galán, S., Francés, F., 2023. Evaluation of ERA5 and ERA5-land reanalysis precipitation datasets over Spain (1951–2020). Atmospheric Res 284, 106606. https://doi.org/10.1016/j.atmosres.2023.106606.
Grissino-Mayer, H.D., Fritts, H.C., 1997. The international tree-ring data bank: an enhanced global database serving the global scientific community. The Holocene 7, 235–238. https://doi.org/10.1177/095968369700700212.
Guiterman, C.H., Gille, E., Shepherd, E., McNeill, S., Payne, C.R., Morrill, C., 2024. The international tree-ring data bank at fifty: status of stewardship for future scientific discovery. Tree-Ring Res 80. https://doi.org/10.3959/TRR2023-2.
Gupta, R., Sharma, L.K., 2019. The process-based forest growth model 3-PG for use in forest management: a review. Ecol. Model. 397, 55–73. https://doi.org/10.1016/j.ecolmodel.2019.01.007.
Härkönen, S., Neumann, M., Mues, V., Berninger, F., Bronisz, K., Cardellini, G., Chirici, G., Hasenauer, H., Koehl, M., Lang, M., Merganicova, K., Mohren, F., Moiseyev, A., Moreno, A., Mura, M., Muys, B., Olschofsky, K., Del Perugia, B., Rørstad, P.K., Solberg, B., Thivolle-Cazat, A., Trotsiuk, V., Mäkelä, A., 2019. A climate-sensitive forest model for assessing impacts of forest management in Europe. Environ. Model. Softw. 115, 128–143. https://doi.org/10.1016/j.envsoft.2019.02.009.
Hare, V.J., Lavergne, A., 2021. Differences in carbon isotope discrimination between angiosperm and gymnosperm woody plants, and their geological significance. Geochim. Cosmochim. Acta 300, 215–230. https://doi.org/10.1016/j.gca.2021.02.029.
Hargreaves, G.H., 1994. Defining and using reference evapotranspiration. J. Irrig. Drain. Eng. 120, 1132–1139.
Horel, J.D., Dong, X., 2010. An evaluation of the distribution of remote automated weather stations (RAWS). J. Appl. Meteorol. Climatol. 49, 1563–1578. https://doi.org/10.1175/2010JAMC2397.1.
Hufkens, K., 2019. ecmwfr: interface to "ECMWF" and "CDS" data Web services. https://doi.org/10.32614/CRAN.package.ecmwfr.
Hunter, J.D., 2007. Matplotlib: a 2D graphics environment. Comput. Sci. Eng. 9, 90–95. https://doi.org/10.1109/MCSE.2007.55.
IPCC, 2023. Climate Change 2022 – Impacts. Adaptation and Vulnerability: Working Group II Contribution to the Sixth Assessment Report of the Intergovernmental Panel On Climate Change, 1st ed. Cambridge University Press. https://doi.org/10.1017/9781009325844.
Jaafar, H.H., Sujud, L.H., 2024. High-resolution satellite imagery reveals a recent accelerating rate of increase in land evapotranspiration. Remote Sens. Environ. 315, 114489. https://doi.org/10.1016/j.rse.2024.114489.
James, G., Witten, D., Hastie, T., Tibshirani, R., others, 2013. An Introduction to Statistical Learning. Springer.
Jeong, J., Barichivich, J., Peylin, P., Haverd, V., McGrath, M.J., Vuichard, N., Evans, M. N., Babst, F., Luyssaert, S., 2021. Using the International Tree-Ring Data Bank (ITRDB) records as century-long benchmarks for global land-surface models. Geosci. Model Dev. 14, 5891–5913. https://doi.org/10.5194/gmd-14-5891-2021.
Jevšenak, J., Klisz, M., Mašek, J., Čada, V., Janda, P., Svoboda, M., Vostarek, O., Treml, V., Van Der Maaten, E., Popa, A., Popa, I., Van Der Maaten-Theunissen, M., Zlatanov, T., Scharnweber, T., Ahlgrimm, S., Stolz, J., Sochová, I., Roibu, C.-C., Pretzsch, H., Schmied, G., Uhl, E., Kaczka, R., Wrzesiński, P., Šenfeldr, M., Jakubowski, M., Tumajer, J., Wilmking, M., Obojes, N., Rybníček, M., Lévesque, M., Potapov, A., Basu, S., Stojanović, M., Stjepanović, S., Vitas, A., Arnič, D., Metslaid, S., Neycken, A., Prislan, P., Hartl, C., Ziche, D., Horáček, P., Krejza, J., Mikhailov, S., Světlík, J., Kalisty, A., Kolář, T., Lavnyy, V., Hordo, M., Oberhuber, W., Levanič, T., Mészáros, I., Schneider, L., Lehejček, J., Shetti, R., Bošeľa, M., Copini, P., Koprowski, M., Sass-Klaassen, U., Izmir, Ş.C., Bakys, R., Entner, H., Esper, J., Janecka, K., Martinez Del Castillo, E., Verbylaite, R., Árvai, M., De Sauvage, J.C., Čufar, K., Finner, M., Hilmers, T., Kern, Z., Novak, K., Ponjarac, R., Puchałka, R., Schuldt, B., Škrk Dolar, N., Tanovski, V., Zang, C., Žmegač, A., Kuithan, C., Metslaid, M., Thurm, E., Hafner, P., Krajnc, L., Bernabei, M., Bojić, S., Brus, R., Burger, A., D'Andrea, E., Đorem, T., Główęda, M., Gričar, J., Gutalj, M., Horváth, E., Kostić, S., Matović, B., Merela, M., Miletić, B., Morgós, A., Paluch, R., Pilch, K., Rezaie, N., Rieder, J., Schwab, N., Sewerniak, P., Stojanović, D., Ullmann, T., Waszak, N., Zin, E., Skudnik, M., Oštir, K., Rammig, A., Buras, A., 2024. Incorporating high-resolution climate, remote sensing and topographic data to map

annual forest growth in central and eastern Europe. Sci. Total Environ. 913, 169692. https://doi.org/10.1016/j.scitotenv.2023.169692.
Kannenberg, S.A., Schwalm, C.R., Anderegg, W.R.L., 2020. Ghosts of the past: how drought legacy effects shape forest functioning and carbon cycling. Ecol. Lett. 23, 891–901. https://doi.org/10.1111/ele.13485.
Keeling, C.D., Piper, S.C., Bacastow, R.B., Wahlen, M., Whorf, T.P., Heimann, M., Meijer, H.A., 2005. Atmospheric $CO_2$ and $^{13}CO_2$ exchange with the terrestrial biosphere and oceans from 1978 to 2000: observations and carbon cycle implications. A History of Atmospheric $CO_2$ and Its Effects On Plants, Animals, and Ecosystems. Springer, pp. 83–113.
Keenan, T.F., Hollinger, D.Y., Bohrer, G., Dragoni, D., Munger, J.W., Schmid, H.P., Richardson, A.D., 2013. Increase in forest water-use efficiency as atmospheric carbon dioxide concentrations rise. Nature 499, 324–327.
Klein Tank, A.M.G., Wijngaard, J.B., Können, G.P., Böhm, R., Demarée, G., Gocheva, A., Mileta, M., Pashiardis, S., Hejkrlik, L., Kern-Hansen, C., Heino, R., Bessemoulin, P., Müller-Westermeier, G., Tzanakou, M., Szalai, S., Pálsdóttir, T., Fitzgerald, D., Rubin, S., Capaldo, M., Maugeri, M., Leitass, A., Bukantis, A., Aberfeld, R., Van Engelen, A.F.V., Forland, E., Mietus, M., Coelho, F., Mares, C., Razuvaev, V., Nieplova, E., Cegnar, T., Antonio López, J., Dahlström, B., Moberg, A., Kirchhofer, W., Ceylan, A., Pachaliuk, O., Alexander, L.V., Petrovic, P., 2002. Daily dataset of 20th-century surface air temperature and precipitation series for the European Climate Assessment. Int. J. Climatol. 22, 1441–1453. https://doi.org/10.1002/joc.773.
Kostić, S., Wagner, W., Orlović, S., Levanič, T., Zlatanov, T., Goršić, E., Kesić, L., Matović, B., Tsvetanov, N., Stojanović, D.B., 2021. Different tree-ring width sensitivities to satellite-based soil moisture from dry, moderate and wet pedunculate oak (*Quercus robur* L.) stands across a southeastern distribution margin. Sci. Total Environ. 800, 149536. https://doi.org/10.1016/j.scitotenv.2021.149536.
Lal, P., Singh, G., Das, N.N., Colliander, A., Entekhabi, D., 2022. Assessment of ERA5-land volumetric soil water layer product using In situ and SMAP soil moisture observations. IEEE Geosci. Remote Sens. Lett. 19, 1–5. https://doi.org/10.1109/LGRS.2022.3223985.
Leuchner, M., Hertel, C., Rötzer, T., Seifert, T., Weigt, R., Werner, H., Menzel, A., 2012. Solar radiation as a driver for growth and competition in forest stands. In: Matyssek, R., Schnyder, H., Oßwald, W., Ernst, D., Munch, J.C., Pretzsch, H. (Eds.), Growth and Defence in Plants, Ecological Studies. Springer Berlin Heidelberg, Berlin, Heidelberg, pp. 175–191. https://doi.org/10.1007/978-3-642-30645-7_8.
Leuschner, C., Ellenberg, H., 2017. Ecology of Central European Forests: Vegetation Ecology of Central Europe, I. Springer International Publishing, Cham. https://doi.org/10.1007/978-3-319-43042-3.
Lexer, M.J., Hönninger, K., 2001. A modified 3D-patch model for spatially explicit simulation of vegetation composition in heterogeneous landscapes. For. Ecol. Manag. 144, 43–65. https://doi.org/10.1016/S0378-1127(00)00386-8.
Manvailer, V., Hamann, A., 2024. Validation of global precipitation time series products against tree ring records and remotely sensed vegetation greenness. PLOS ONE 19, e0299111. https://doi.org/10.1371/journal.pone.0299111.
Martínez-Fernández, J., Almendra-Martín, L., De Luis, M., González-Zamora, A., Herrero-Jiménez, C., 2019. Tracking tree growth through satellite soil moisture monitoring: a case study of *Pinus halepensis* in Spain. Remote Sens. Environ. 235, 111422. https://doi.org/10.1016/j.rse.2019.111422.
Monteith, J.L., 1965. Evaporation and environment. Symposia of the Society for Experimental Biology. Cambridge University Press (CUP), Cambridge, pp. 205–234.
Muñoz-Sabater, J., Dutra, E., Agustí-Panareda, A., Albergel, C., Arduini, G., Balsamo, G., Boussetta, S., Choulga, M., Harrigan, S., Hersbach, H., Martens, B., Miralles, D.G., Piles, M., Rodríguez-Fernández, N.J., Zsoter, E., Buontempo, C., Thépaut, J.-N., 2021. ERA5-Land: a state-of-the-art global reanalysis dataset for land applications. Earth Syst. Sci. Data 13, 4349–4383. https://doi.org/10.5194/essd-13-4349-2021.
NOAA, 2025. Pale Data Search. National Centers For Environmental Information.
Norby, R.J., DeLucia, E.H., Gielen, B., Calfapietra, C., Giardina, C.P., King, J.S., Ledford, J., McCarthy, H.R., Moore, D.J.P., Ceulemans, R., De Angelis, P., Finzi, A.C., Karnosky, D.F., Kubiske, M.E., Lukac, M., Pregitzer, K.S., Scarascia-Mugnozza, G.E., Schlesinger, W.H., Oren, R., 2005. Forest response to elevated $CO_2$ is conserved across a broad range of productivity. Proc. Natl. Acad. Sci. 102, 18052–18056. https://doi.org/10.1073/pnas.0509478102.
Nwayor, I.J., Robeson, S.M., 2024. Exploring the relationship between SPI and SPEI in a warming world. Theor. Appl. Climatol. 155, 2559–2569. https://doi.org/10.1007/s00704-023-04764-y.
Obladen, N., Dechering, P., Skiadaresis, G., Tegel, W., Keßler, J., Höllerl, S., Kaps, S., Hertel, M., Dulamsuren, C., Seifert, T., Hirsch, M., Seim, A., 2021. Tree mortality of European beech and Norway spruce induced by 2018-2019 hot droughts in central Germany. Agric. For. Meteorol. 307, 108482. https://doi.org/10.1016/j.agrformet.2021.108482.
Obojes, N., Buscarini, S., Meurer, A.K., Tasser, E., Oberhuber, W., Mayr, S., Tappeiner, U., 2024. Tree growth at the limits: the response of multiple conifers to opposing climatic constraints along an elevational gradient in the Alps. Front. For. Glob. Change 7, 1332941. https://doi.org/10.3389/ffgc.2024.1332941.
Ols, C., Klesse, S., Girardin, M.P., Evans, M.E.K., DeRose, R.J., Trouet, V., 2023. Detrending climate data prior to climate–growth analyses in dendroecology: a common best practice? Dendrochronologia 79, 126094. https://doi.org/10.1016/j.dendro.2023.126094.
Oogathoo, S., Duchesne, L., Houle, D., Kneeshaw, D., Bélanger, N., 2024. Precipitation and relative humidity favours tree growth while air temperature and relative humidity respectively drive winter stem shrinkage and expansion. Front. For. Glob. Change 7, 1368590. https://doi.org/10.3389/ffgc.2024.1368590.
Paulsen, J., Weber, U.M., Körner, Ch., 2000. Tree growth near treeline: abrupt or gradual reduction with altitude? Arct. Antarct. Alp. Res. 32, 14–20. https://doi.org/10.1080/15230430.2000.12003334.
Pedregosa, F., Varoquaux, G., Gramfort, A., Michel, V., Thirion, B., Grisel, O., Blondel, M., Prettenhofer, P., Weiss, R., Dubourg, V., Vanderplas, J., Passos, A., Cournapeau, D., Brucher, M., Perrot, M., Duchesnay, E., 2011. Scikit-learn: machine learning in Python. J. Mach. Learn. Res. 12, 2825–2830.
Pelosi, A., Bolognesi, S.F., D'Urso, G., Chirico, G.B., 2021. Assessing crop evapotranspiration by combining ERA5-land meteorological reanalysis data and visible and near-infrared satellite imagery. 2021 IEEE International Workshop On Metrology for Agriculture and Forestry (MetroAgriFor). Trento-Bolzano, Italy, pp. 285–289. https://doi.org/10.1109/MetroAgriFor52389.2021.9628640.
Quast, R., Wagner, W., Bauer-Marschallinger, B., Vreugdenhil, M., 2023. Soil moisture retrieval from Sentinel-1 using a first-order radiative transfer model—A case-study over the Po-Valley. Remote Sens. Environ. 295, 113651. https://doi.org/10.1016/j.rse.2023.113651.
R Core Team, 2024. R: a language and environment for Statistical Computing. R Foundation for Statistical Computing, Vienna, Austria.
Raybaut, P., 2009. Spyder-documentation.
Roderick, M.L., Greve, P., Farquhar, G.D., 2015. On the assessment of aridity with changes in atmospheric $CO_2$. Water Resour. Res. 51, 5450–5463. https://doi.org/10.1002/2015WR017031.
Sabatini, F., 2017. Setting up and managing automatic weather stations for remote sites monitoring: from Niger to Nepal. In: Tiepolo, M., Pezzoli, A., Tarchiani, V. (Eds.), Renewing Local Planning to Face Climate Change in the Tropics, Green Energy and Technology. Springer International Publishing, Cham, pp. 21–39. https://doi.org/10.1007/978-3-319-59096-7_2.
Sanmiguel-Vallelado, A., Camarero, J.J., Morán-Tejeda, E., Gazol, A., Colangelo, M., Alonso-González, E., López-Moreno, J.I., 2021. Snow dynamics influence tree growth by controlling soil temperature in mountain pine forests. Agric. For. Meteorol. 296, 108205. https://doi.org/10.1016/j.agrformet.2020.108205.
Schönauer, M., Asabere, S.B., Sauer, D., Drollinger, S., 2025. Topographic indices and ERA5-Land data to describe soil moisture variability in a Central European beech forest. J. Hydrol. Reg. Stud. 59, 102456. https://doi.org/10.1016/j.ejrh.2025.102456.
Schreiber-Gregory, D.N., 2018. Ridge regression and multicollinearity: an in-depth review. Model Assist. Stat. Appl. 13, 359–365. https://doi.org/10.3233/MAS-180446.
Schweingruber, F.H., 2007. Wood Structure and Environment, Springer Series in Wood Science. Springer Berlin Heidelberg, Berlin, Heidelberg. https://doi.org/10.1007/978-3-540-48548-3.
Schweingruber, F.H., 2012. Tree rings: Basics and Applications of Dendrochronology. Springer Science & Business Media.
Sedjo, R., Sohngen, B., 2012. Carbon sequestration in forests and soils. Annu. Rev. Resour. Econ. 4, 127–144. https://doi.org/10.1146/annurev-resource-083110-115941.
Senf, C., Buras, A., Zang, C.S., Rammig, A., Seidl, R., 2020. Excess forest mortality is consistently linked to drought across Europe. Nat. Commun. 11, 6200. https://doi.org/10.1038/s41467-020-19924-1.
Serra-Maluquer, X., Gazol, A., Anderegg, W.R.L., Martínez-Vilalta, J., Mencuccini, M., Camarero, J.J., 2022. Wood density and hydraulic traits influence species' growth response to drought across biomes. Glob. Change Biol. 28, 3871–3882. https://doi.org/10.1111/gcb.16123.
Silva, L.C.R., Anand, M., Leithead, M.D., 2010. Recent widespread tree growth decline despite increasing atmospheric $CO_2$. PLoS ONE 5, e11543. https://doi.org/10.1371/journal.pone.0011543.
Speer, J., 2009. Fundamentals of Tree-Ring Research. University of Arizona Press.
Stull, R.B., 2012. An Introduction to Boundary Layer Meteorology. Springer Science & Business Media.
Swann, A.L.S., Hoffman, F.M., Koven, C.D., Randerson, J.T., 2016. Plant responses to increasing $CO_2$ reduce estimates of climate impacts on drought severity. Proc. Natl. Acad. Sci. 113, 10019–10024. https://doi.org/10.1073/pnas.1604581113.
Sweet, L., Müller, C., Anand, M., Zscheischler, J., 2023. Cross-validation strategy impacts the performance and interpretation of machine learning models. Artif. Intell. Earth Syst. 2, e230026. https://doi.org/10.1175/AIES-D-23-0026.1.
Tang, R., Peng, Z., Liu, M., Li, Z.-L., Jiang, Y., Hu, Y., Huang, L., Wang, Y., Wang, J., Jia, L., Zheng, C., Zhang, Y., Zhang, K., Yao, Y., Chen, X., Xiong, Y., Zeng, Z., Fisher, J.B., 2024. Spatial-temporal patterns of land surface evapotranspiration from global products. Remote Sens. Environ. 304, 114066. https://doi.org/10.1016/j.rse.2024.114066.
Thom, D., Buras, A., Heym, M., Klemmt, H.-J., Wauer, A., 2023. Varying growth response of Central European tree species to the extraordinary drought period of 2018–2020. Agric. For. Meteorol. 338, 109506. https://doi.org/10.1016/j.agrformet.2023.109506.
Vaganov, E.A., Hughes, M.K., Kirdyanov, A.V., Schweingruber, F.H., Silkin, P.P., 1999. Influence of snowfall and melt timing on tree growth in subarctic Eurasia. Nature 400, 149–151. https://doi.org/10.1038/22087.
Vicente-Serrano, S.M., Beguería, S., López-Moreno, J.I., 2010. A multiscalar drought index sensitive to global warming: the standardized precipitation evapotranspiration index. J. Clim. 23, 1696–1718. https://doi.org/10.1175/2009JCLI2909.1.
Vicente-Serrano, S.M., Camarero, J.J., Azorin-Molina, C., 2014. Diverse responses of forest growth to drought time-scales in the Northern Hemisphere. Glob. Ecol. Biogeogr. 23, 1019–1030. https://doi.org/10.1111/geb.12183.
Virtanen, P., Gommers, R., Oliphant, T.E., Haberland, M., Reddy, T., Cournapeau, D., Burovski, E., Peterson, P., Weckesser, W., Bright, J., van der Walt, S.J., Brett, M., Wilson, J., Millman, K.J., Mayorov, N., Nelson, A.R.J., Jones, E., Kern, R., Larson, E.,

Carey, C.J., Polat, İ., Feng, Y., Moore, E.W., VanderPlas, J., Laxalde, D., Perktold, J., Cimrman, R., Henriksen, I., Quintero, E.A., Harris, C.R., Archibald, A.M., Ribeiro, A. H., Pedregosa, F., van Mulbregt, P., SciPy 1.0 Contributors, 2020. SciPy 1.0: fundamental algorithms for scientific computing in Python. Nat. Methods 17, 261–272. https://doi.org/10.1038/s41592-019-0686-2.

Wang, Z., Guan, M., Fang, W., Yuan, S., Cao, P., Jiang, Y., 2024. Applicability assessment of ERA5-land temperature data in the research of the relationship between tree rings and climate in China. Quaternary Sciences 44, 1031–1043. https://doi.org/10.11928/j.issn.1001-7410.2024.04.16.

Waskom, M., 2021. seaborn: statistical data visualization. J. Open Source Softw. 6, 3021. https://doi.org/10.21105/joss.03021.

Way, D.A., Montgomery, R.A., 2015. Photoperiod constraints on tree phenology, performance and migration in a warming world. Plant Cell Environ 38, 1725–1736. https://doi.org/10.1111/pce.12431.

Way, D.A., Oren, R., 2010. Differential responses to changes in growth temperature between trees from different functional groups and biomes: a review and synthesis of data. Tree Physiol 30, 669–688. https://doi.org/10.1093/treephys/tpq015.

Weiner, J., Thomas, S.C., 2001. The nature of tree growth and the "age-related decline in forest productivity. Oikos 94, 374–376. https://www.jstor.org/stable/3547583.

Western Regional Climate Center, 2008. IHOP_2002: USFS Remote Automatic Weather Station (RAWS) Data. Version 1.0. https://doi.org/10.26023/9QFQ-P3MA-MB0E.

Wigley, T.M.L., Briffa, K.R., Jones, P.D., 1984. On the average value of correlated time series, with applications in dendroclimatology and hydrometeorology. J. Clim. Appl. Meteorol. 23, 201–213. https://doi.org/10.1175/1520-0450(1984)023<0201:OTAVOC>2.0.CO;2.

WMO, 2023. Guide to Meteorological Instruments and Methods of Observation. World Meteorological Organization, Geneva.

Wong, C.Y.S., Young, D.J.N., Latimer, A.M., Buckley, T.N., Magney, T.S., 2021. Importance of the legacy effect for assessing spatiotemporal correspondence between interannual tree-ring width and remote sensing products in the Sierra Nevada. Remote Sens. Environ. 265, 112635. https://doi.org/10.1016/j.rse.2021.112635.

Wu, X., Liu, H., Hartmann, H., Ciais, P., Kimball, J.S., Schwalm, C.R., Camarero, J.J., Chen, A., Gentine, P., Yang, Y., Zhang, S., Li, X., Xu, C., Zhang, W., Li, Z., Chen, D., 2022. Timing and order of extreme drought and wetness determine bioclimatic sensitivity of tree growth. Earths Future 10. https://doi.org/10.1029/2021EF002530 e2021EF002530.

Xing, Z., Li, X., Fan, L., Colliander, A., Frappart, F., De Rosnay, P., Fernandez-Moran, R., Liu, X., Wang, H., Zhao, L., Wigneron, J.-P., 2023. Assessment of 9 km SMAP soil moisture: evidence of narrowing the gap between satellite retrievals and model-based reanalysis. Remote Sens. Environ. 296, 113721. https://doi.org/10.1016/j.rse.2023.113721.

Zhang, H., Tang, B.-H., Li, Z.-L., 2024. A practical two-step framework for all-sky land surface temperature estimation. Remote Sens. Environ. 303, 113991. https://doi.org/10.1016/j.rse.2024.113991.

Zhao, S., Pederson, N., D'Orangeville, L., HilleRisLambers, J., Boose, E., Penone, C., Bauer, B., Jiang, Y., Manzanedo, R.D., 2019. The International Tree-Ring Data Bank (ITRDB) revisited: data availability and global ecological representativity. J. Biogeogr. 46, 355–368. https://doi.org/10.1111/jbi.13488.

Zweifel, R., Sterck, F., 2018. A conceptual tree model explaining legacy effects on stem growth. Front. For. Glob. Change 1, 9. https://doi.org/10.3389/ffgc.2018.00009.